Helicopter Response to an Airplane's Trailing Vortex

Wayne R. Mantay,* G. Thomas Holbrook,* Richard L. Campbell,* and Robert L. Tomaine*
NASA Langley Research Center, Hampton, Va.

A flight investigation was conducted to determine quantitatively the response of a medium-weight helicopter to the trailing-vortex system of a fixed-wing aircraft. Both flight tests and analytical tools were utilized in the investigation. The flight tests involved an extensively instrumented UH-1H helicopter and a C-54 aircraft. Penetrations of the vortex system by the UH-1H were made at the following nominal conditions: the C-54 flew at 5500-ft alt at a nominal gross weight of 58,000 lb and an indicated airspeed of 115 knots in a cruise configuration; the UH-1H, nominally 7200-lb gross weight, flew at 60-knots indicated airspeed during the penetrations at separation distances of 6.64 naut miles to 0.42 naut mile between aircraft. In general, the data analyzed for these tests indicated that no unsafe penetration occurred. Further, penetrating vehicle attitude changes and structural loads were nominal. In addition, the response of the helicopter did not change appreciably with decreased separation distance.

Nomenclature

I_{xx} = roll moment of inertia, slug-ft^2
I_{yy} = pitch moment of inertia, slug-ft^2
I_{zz} = yaw moment of inertia, slug-ft^2
K_c = core size factor—determined from vehicle separation distance and effective viscosity, ft^2
R_E = distance from center of vortex system to start of vortex field, ft
R_{IN} = distance from center of vortex system to area where rotorcraft is completely within vortex velocity field, ft
t = maneuver time, sec
$X_{c.g.}$ = longitudinal center-of-gravity location, in.
$Y_{c.g.}$ = lateral center-of-gravity location, in.
$Z_{c.g.}$ = vertical center-of-gravity location, in.
α = measured angle of attack, deg
β = measured sideslip angle, deg
Γ = vortex circulation strength, ft^2/sec
ΔX_c = separation between vortex centers, ft
θ = aircraft pitch attitude, deg
ϕ = aircraft roll attitude, deg

I. Introduction

WAKE-VORTEX encounters have caused restrictions to be placed on separation distances for multiple aircraft use of the terminal area. The data upon which the separation distances are based were derived in part from flight tests of fixed-wing aircraft.[1] The increasing number of rotary-wing aircraft used in the terminal area provided the impetus to investigate the penetration of a vortex wake by a rotorcraft.

A flight investigation[2] was conducted to determine quantitatively, for the first time, the response of a medium-weight helicopter to the trailing vortex system of a fixed-wing aircraft. Such a penetration is shown schematically in Fig. 1. In addition to providing a large data matrix, the flight tests also afford an indication of potential problem areas that may exist for helicopter penetrations of a fixed-wing trailing vortex system. This series of tests was undertaken to provide an initial definition of the safe-flight envelope for this particular helicopter/fixed-wing combination.

Presented at the AIAA 3rd Atmospheric Flight Mechanics Conference, Arlington, Texas, June 7-9, 1976 (in bound volume of Conference papers, no paper number); submitted June 28, 1976; revision received Nov. 29, 1976.

Index categories: Aircraft Flight Operations; VTOL Flight Operations; VTOL Handling, Stability, and Control.

*Aerospace Technologist.

II. Method of Approach

Both flight tests and analytical tools where used in the investigation. The flight tests involved a C-54 aircraft and an extensively instrumented UH-1H helicopter. State-of-the-art instrumentation, real-time data systems, and safety hardware and software were incorporated in the flight program. The use of these systems allowed, for the first time, a systematic and controlled investigation of the response of a rotary-wing vehicle to a vortex system, the nature of which might be encountered in the terminal area.

Description of Flight Vehicles

Test Helicopter

A UH-1H helicopter was the penetrating vehicle for these tests. As shown in Fig. 2, it was equipped with both optical

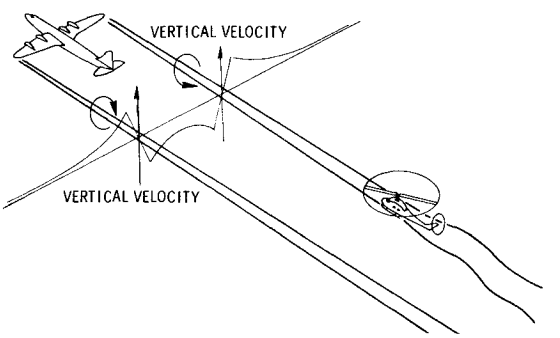

Fig. 1 Schematic of vortex wake intercept by a helicopter.

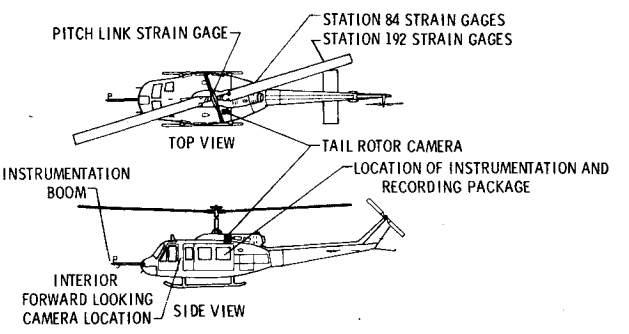

Fig. 2 UH-1H test helicopter.

Table 1 Helicopter main rotor system description

Type of hub	Teetering
Rotor radius	24 ft
Blade chord	21in.
Blade airfoil	0012
Blade twist (root to tip)	−10.9° linear
Precone angle	2.375°
Number of blades	2
Rotor rotational speed	324 rpm

data hardware and electronic data systems. The aircraft was nominally 7200 lb with a horizontal center-of-gravity location 7 in. aft of the main rotor hub. It is powered by a gas turbine of 1400 shaft horsepower. The characteristics of its main rotor system are given in Table 1.

Vortex Generating Aircraft

The C-54 aircraft shown in Fig. 3 generated the vortex wake, which the helicopter penetrated. This aircraft was nominally 58,000 lb gross weight. It was equipped with a vortex marking system, which used chalk dust to aid in visualizing the wing vortex system. The wing span, aspect ratio, and other geometric parameter values are indicated in Fig. 3. A rough comparison can be made between the vortex wake strengths of the C-54 and current passenger aircraft by taking the ratio of their bound circulation at equivalent cruise conditions. This ratio indicated a higher circulation for current aircraft by a factor ranging from about 2 for a DC-9 up to about 7 for a 747.

Description of Instrumentation

The penetrating aircraft was instrumented to record the data parameters in Table 2. In addition, several critical parameters were telemetered real-time to a safety-of-flight station on the ground, and separation distance between aircraft was displayed onboard the UH-1H. After each test flight, the data were processed digitally and combined to yield parameters such as airspeed and main rotor blade structural loads.

Test Procedure

Penetrations of the vortex system by the UH-1H were made at the following nominal conditions: the C-54 flew at 5500-ft

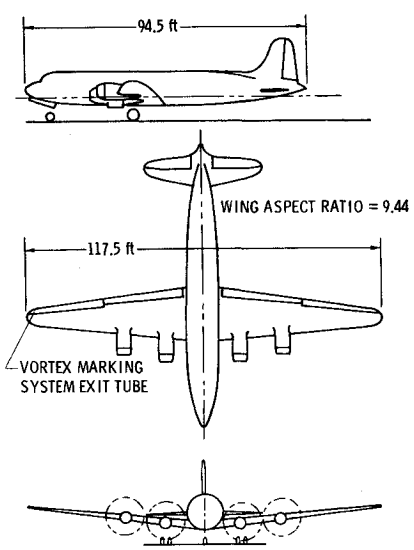

Fig. 3 C-54 test aircraft.

alt in a cruise configuration, at a gross weight of 58,000 lb and an indicated airspeed of 115 knots. The UH-1H, nominally 7200 lb gross weight, flew at 60 knots indicated airspeed during the penetrations at separation distances of 6.64 naut miles to 0.42 naut mile between aircraft.

The vortex penetration was initiated by a C-54 flyby at altitude with the wing-tip vortex marked by a chalk dust trail as shown in Fig. 4. The starboard wing-tip vortex, thus marked, was penetrated by the helicopter when the appropriate separation distance between aircraft was reached, as indicated by the onboard range measurement system. The flight program was begun at a large separation distance, where the vortex wake began dissipating. Subsequent runs closed the separation distance systematically.

Each oblique penetration of the tip vortex was made from the lower right side of the C-54 wake, ascending up through the vortex, followed by several descents and ascents through the tip vortex as it aged. Figure 5 shows the UH-1H during an ascent through the vortex at a separation distance of about 3.5 naut miles. The oblique penetrations were made predominantly at nonstick-fixed conditions.

III. Discussion of Flight Results

As previously mentioned, real-time telemetry data provided safety-of-flight information pertaining to critical aircraft parameters. Recorded data which included all real-time information, vehicle aerodynamic state, accelerations, attitudes, and aircraft separation. In addition, main rotor mechanical data, structural loads, and tail rotor flapping were recorded.

Figures 6-9 present some pertinent flight data. Figures 6 and 7 are time histories of vehicle and main rotor blade response, respectively. Figure 8 is a compilation of main rotor blade loading data. In an effort to correlate the cause and effect of vortex penetration and vehicle response, Figs. 9a-e are presented. These cross plots indicate the trend of helicopter response with other aircraft parameters, including tail rotor flapping.

Table 2 Flight data parameters

Parameter	Sensor
Three vehicle attitudes	Gyro
Three angular rates	Gyro
Three linear accelerations	Accelerometer
Four control inputs	Transducer
Angle of attack	Vane/potentiometer
Angle of sideslip	Vane/potentiometer
Main rotor blade angle	Control position transducer
Main rotor azimuth	Shaft endcoder
Total temperature	Hot wire
Static/differential pressure	Pressure transducer
Main rotor speed	Magnetic counter
Engine torque pressure (UH-1H)	Pressure transducer
Rate of climb	Inertial vertical speed indicator
Chordwise bending moment at stations 84 and 192 on main rotor blade	Strain gage
Flapwise bending moment at stations 84 and 192 on main rotor blade	Strain gage
Rotating pitch link load	Strain gage
Time code	36-bit time code generator
Aircraft separation distance	Transponder and interrogator/receiver

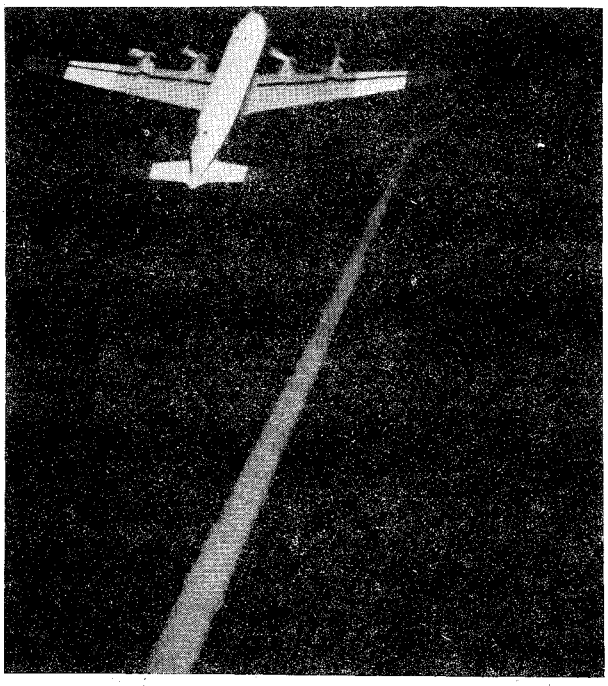

Fig. 4 Marking the wing-tip vortex.

Fig. 5 Test helicopter ascending through vortex wake of C-54.

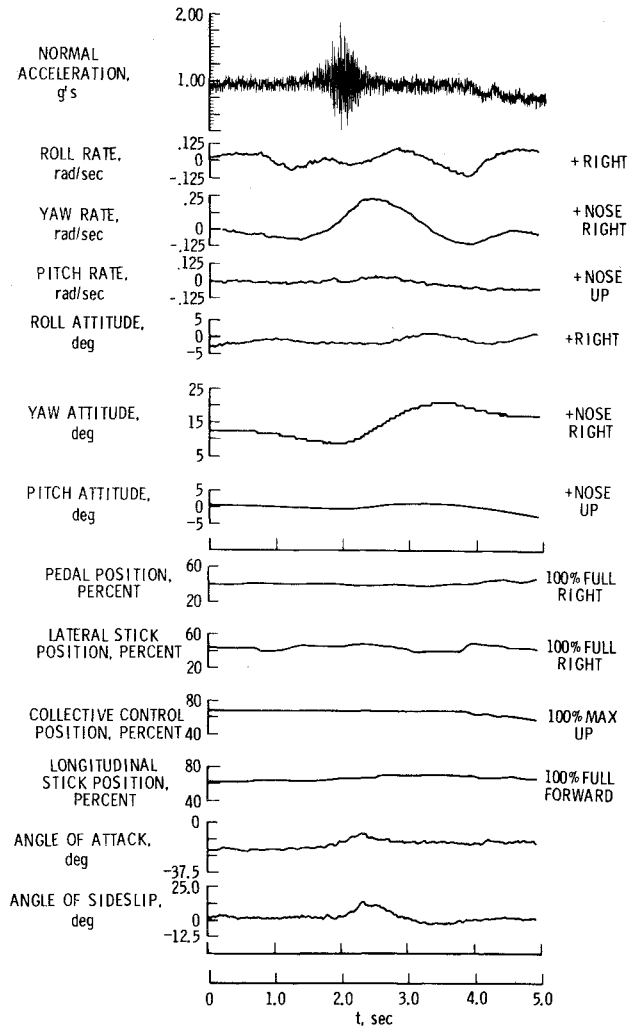

Fig. 6 Typical time history of helicopter response to vortex wake of C-54.

Vehicle Attitude Response

Figure 6 shows a typical time history of the data obtained from one of 132 penetrations of the C-54 vortex wake. The vortex was penetrated by the fuselage boom at $t=2.3$ sec, as can be seen from the α and β outputs of Fig. 6. The separation between aircraft for this penetration was 2.95 naut miles. This particular penetration was made in the nonstick-fixed mode at a helicopter airspeed of 53 knots. The response of the aircraft to the vortex is shown by the time history attitudes, rates, and acceleration.

Data such as those shown in Fig. 6 indicate that the helicopter experiences minimal response when penetrating the vortex wake. The response that does occur is, with the exception of yaw, because of the stick inputs used to maneuver the aircraft and position it correctly for a vortex penetration. This is generally true for all nonstick-fixed penetrations tested, and it can be substantiated by observing the time correlation between stick motions and rates and attitudes, as shown in time histories such as Fig. 6. Except for yaw motions, the vehicle is responding to stick inputs, so that roll and pitch vehicle motions are a function of maneuvering stick inputs, and not a result of vortex perturbations during each penetration. Further substantiation for the cause of motion that does occur before and during a penetration can be obtained through data such as those shown in Fig. 9 a-c. With the exception of yaw, attitude changes correlate well with their respective control inputs, thereby supporting the conclusion drawn for the time history data.

In order to put the helicopter attitude response in perspective, a comparison with fixed-wing response to a vortex wake may be in order. A small general aviation aircraft, of 2225 lb gross weight, was used in a similar vortex encounter investigation.[3] The vortex generating aircraft for that study was identical to that used during this test. The ratios of control sensitivity to vehicle inertia for the light plane of Ref. 3 at 60 knots indicated airspeed, and the ratios for the helicopter described herein were similar. Upon encountering the vortex wake at a separation distance of 3.9 naut miles, and at an indicated airspeed of 90 knots, the general aviation aircraft experienced severe attitude upset. The helicopter, as described previously, experienced minimal response at the same separation distance.

The correlation of yaw motion with pedal, as shown in Fig. 9c, is low. Even though the helicopter yaw motion was minimal during penetration, apparently it was not because of pedal input. It is believed that the nominal yaw motion of the helicopter was caused by the aerodynamic perturbation of the vortex, possibly against the vertical fin of the helicopter (11.6 ft^2 in lateral-projected area). Another cause of the small yaw motion of the helicopter during vortex penetration may be caused by a change in tail rotor loading. This possibility is considered later in this paper.

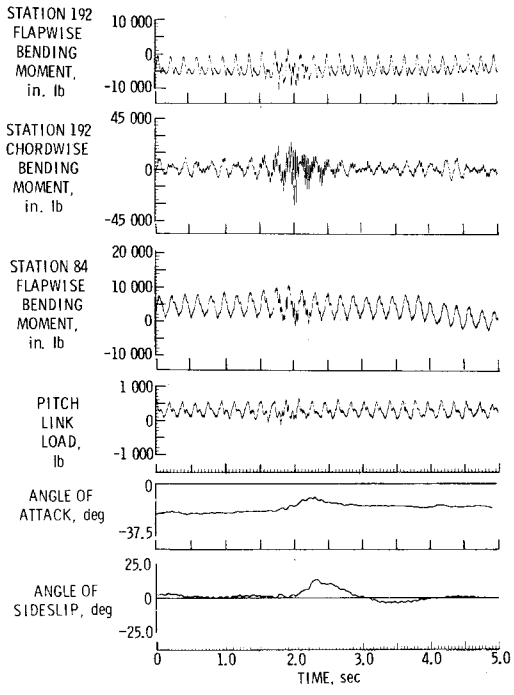

Fig. 7 Main rotor loads time history during vortex encounter.

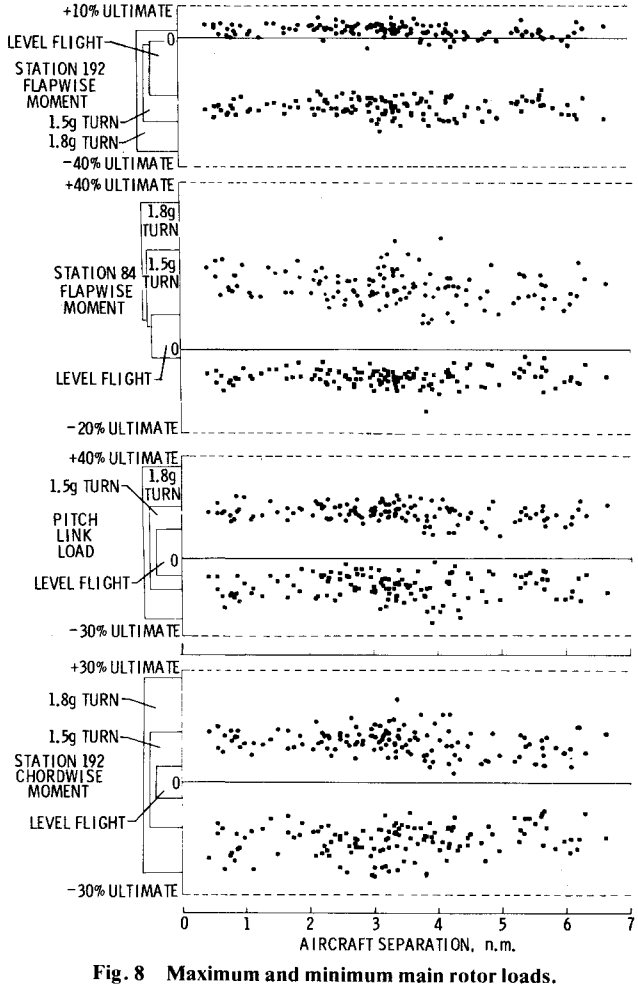

Fig. 8 Maximum and minimum main rotor loads.

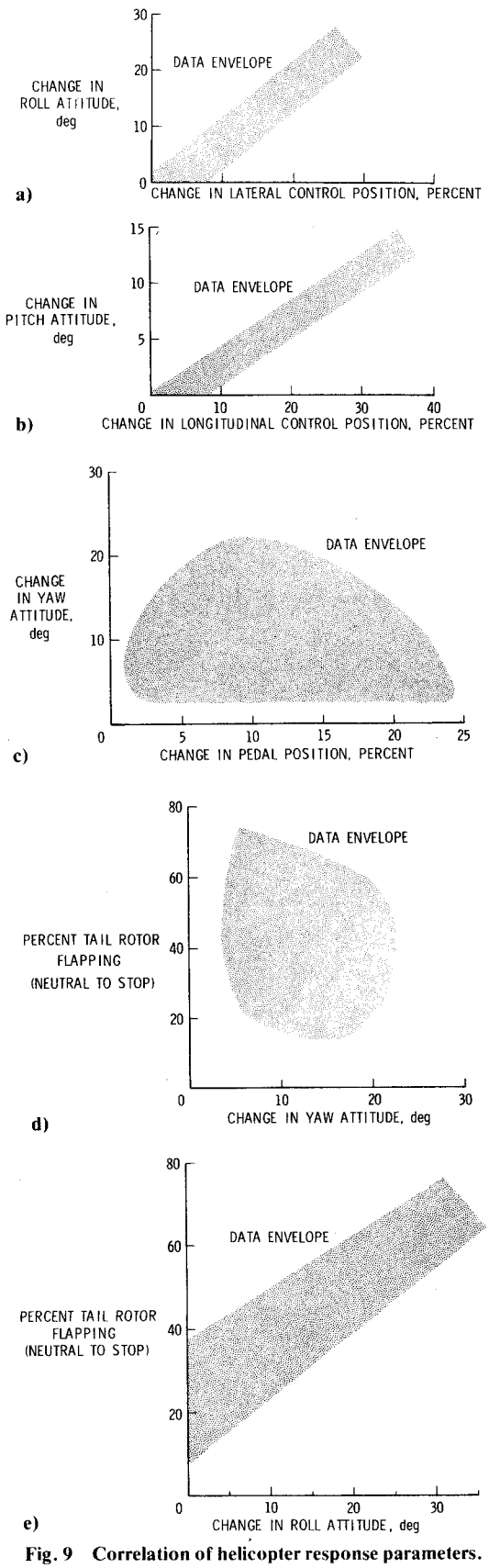

Fig. 9 Correlation of helicopter response parameters.

Main Rotor Loads/Blade Response

Rotor loads are visibly influenced by the vortex encounter, as shown in Fig. 7. These data are representative of the perturbation of rotor loads by the vortex wake and, specifically, occur at 2.95-naut-miles separation at an airspeed of 53 knots. The rotor tip-path plane intercepts the vortex at $t = 2.0$ sec, and the resulting encounter expands the envelope of blade loads as shown. The harmonic content of each blade load sensor output does not change appreciably; only the magnitude does.

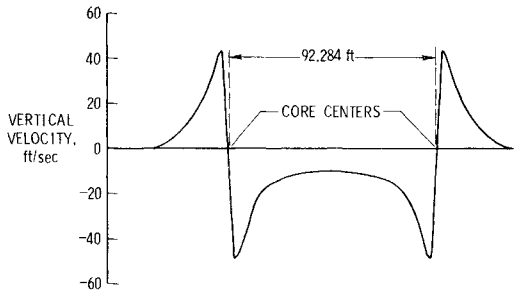

Fig. 10 Simulated trailing vortex system.

In order to put the blade loads increase in perspective, Fig. 8 presents the maximum and minimum values of rotor loads obtained for each penetration. These maximum magnitude values were extracted from the envelope of each load time history, such as Fig. 7. The maximum and minimum rotor loads at the indicated blade stations experienced in various nonvortex-penetrating maneuvers are included in Fig. 8 for comparison.

The flight-test data presented in Figs. 7 and 8 indicate several aspects of blade loads. It is evident that the increase in load envelope during a vortex penetration is nominal with respect to the normal operating envelope of this helicopter. Also, the maximum amplitude for critical blade and control system loads does not change appreciably with vehicle separation distance. These trends indicate that the main rotor blades are responding to an energy source whose integrated effect on the rotor disk is a small change in the blade loading, probably through local angle-of-attack changes at each rotor station. The core diameter of the tip vortex is of the order of magnitude of 1 meter. Although it is true that the peak core velocity of the trailing tip vortex dissipates with age, the total energy in the vortex integrated over the main rotor disk is approximately a constant. Therefore, the integrated effect of the vortex field could be expected to perturb the rotor only by an amount that varies little with changes in the vortex structure as it ages. The data of Fig. 8 lend support to this hypothesis.

As the rotor intercepts the trailing vortex wake, the harmonic content of the rotor/control loads does not change appreciably, as shown by Fig. 7. This indicated that no higher harmonics are excited by the vortex flow. These data do not dismiss the possibility that a resonant condition exists in blade response during vortex penetration. In order to answer this question directly, several penetrations were made in which the helicopter remained in the vortex wake, rather than passing through it. The blade response was similar to that of Fig. 7 in that the load envelope expanded during the rotor's immersion in the vortex and decreased to its nominal level after the helicopter once again returned to an ambient flight condition. The increase in rotor loads, which is well within the operating and safety limits of the rotor system tested, apparently is caused by a direct applied load provided by the vortex wake.

Tail Rotor Response

The possibility of excursions in yaw motion being caused directly by large changes in tail rotor loading has been considered. Large changes in tail rotor loading may manifest themselves by large flapping excursions of the tail rotor, if the tail rotor is highly loaded and accompanied by vehicle angular motions.[4] Significant flapping motions were observed via a high-speed camera. The location of this camera is shown in Fig. 2. These flapping motions generally occurred as a result of the penetration approach roll maneuver, it is believed, and not during the vortex penetration. This can be substantiated as follows: Fig. 9d shows a rather low correlation between tail rotor flapping and yaw attitude excursions, whereas Fig.9e indicates a fairly strong correlation between roll excursions

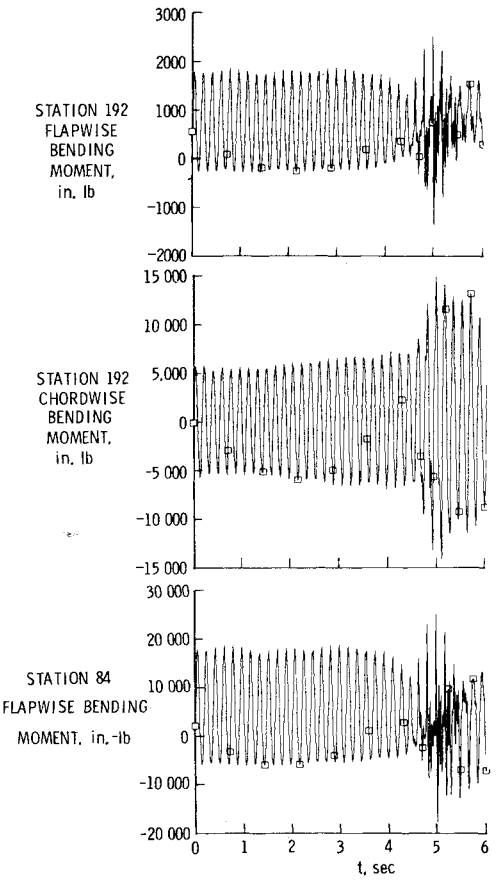

Fig. 11 Analytically predicted main rotor blade response to vortex penetration.

and tail rotor flapping during the data runs. It has been indicated earlier in this paper that large roll attitude excursions were caused by lateral stick inputs during maneuvering in order to position the heliocopter correctly for vortex penetrations. In addition, the tail rotor flapping film did not shown rapid changes in flapping as the chalk dust marking the vortex core passed over the tail rotor disk. Hence, the tail rotor flapping experienced was due to pilot inputs independent of vortex perturbation. These data also indicate that the yaw excursions, which were caused by the vortex, did not originate from tail rotor thrust excursions from a highly loaded tail rotor. Tail rotor thrust excursions in a lightly loaded rotor, or some other aerodynamic vehicle torque imbalance, such as vertical fin force excursions, may be the cause of the yaw motion.

IV. Comparison of Flight Data with Analytical Results

Two computer programs were used during the flight investigation. The first of these, a performance/stability program, provided safety information before the flight program was initiated. This computer program is comprised of a rigid-blade model, whose equations are formulated after Ref. 5. The output from this program predicted transient flapping motions for both tail rotor and main rotor. The calculated values of flapping for both rotors were found to be small when the vortex field was imposed on the helicopter.

A simulation of the C-54 vortex interception by the UH-1H was performed utilizing a rotorcraft flight simulation digital computer program.[6] This program is a general-purpose rotorcraft flight simulation computer program with three basic functions: computing steady-state trim attitudes and control settings, computing vehicle dynamic stability characteristics, and computing vehicle response and blade loadings due to an external disturbance or control input.

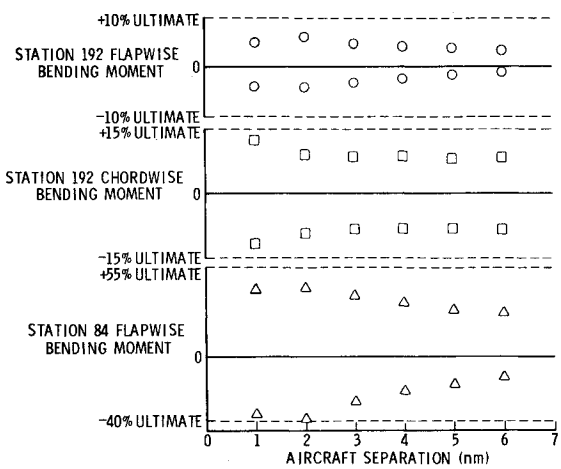

Fig. 12 Predicted maximum and minimum main rotor loads.

The program has various options in each of these basic functions; the rotor can be assumed quasistatic or time variant in either the trim or maneuver execution, and can include blade elasticity. The steady-state trim can be steady level flight, a banked turn, or a constant rate of climb or descent. The external disturbance can take the form of 27 specific effects, including interception of a trailing vortex system. The trailing vortex system consists of two equal-strength, counter-rotating vortices, fixed in the ground reference plane, as shown in Fig. 10. This simulated vortex flowfield is for a separation distance of 3.0 naut miles. The circulation strength of the tip vortex (Γ) was theoretically determined, whereas the core size factor (K_c) was empirically determined.

The program inputs required are substantial, including fuselage and control surface geometry and aerodynamics; rotor geometry, and aerodynamics and elastic characteristics (e.g., blade mode shapes and frequencies); vehicle weights, inertias, control system characteristics, and flight condition.

Thus, all inputs required are not provided herein; however, Table 3 contains the specific inputs that differentiate these runs from a typical UH-1H simulation. Rotor aerodynamics were provided by a NACA 0012 airfoil table, and five fully coupled main rotor blade mode shapes were supplied from another digital computer program[7] for the UH-1H rotor system. The program execution options consisted of a steady-state trim at a specified rate of climb, a time-variant main rotor trim, followed by a time-variant maneuver.

Simulation Procedures

The digital simulation procedure was performed to match the general conditions during flight testing. The vehicle was trimmed 80 ft below the right-wing vortex core, with a 15-fps rate of climb at 60 knots indicated airspeed. This procedure represents a nominal vortex intercept condition, not a specific data flight simulation, since the actual airspeed, rate of climb, and attitude at vortex impact could not be duplicated readily by use of this computer program.

Simulation Results

Simulations for several separation distances were performed using the rotorcraft simulation program. In general, the predicted vehicle response compared favorably with flight-test results, and blade loadings were representative of measured values, but, with the exception of inboard flapwise loading, generally were conservative.

The analytically predicted response of the main rotor blades to the vortex system of Fig. 10 is shown in Fig. 11. The vortex penetration occurs at $t=5$ sec on this figure. The rotor loads are seen to expand as the helicopter obliquely encounters the vortex at this separation distance. The magnitude and harmonic content of the blade response predicted during vortex penetration compare favorably with that of the flight data shown in Fig. 7 for the same flight condition. The lower harmonic content of blade loads before penetration, as shown on Fig. 11, is caused by large computation steps before vortex core intercept to save computer time. It may be noted in Fig. 12 that, with the exception of inboard flapwise loading, the predicted blade loads and vehicle response did not vary appreciably with separation distance, a trend that the flight data also indicated. Table 4 compares the maximum vortex-induced helicopter response in flight to that predicted by the simulation program.

Table 3 Simulation input parameters

Vehicle		Vortex system		Trim flight conditions	
Gross weight	7,77 lb	Γ	1,476.8 ft^2/sec	Indicated airspeed	60 knots
I_{xx}	2,800 slug-ft^2	R_{IN}	58.352 ft	True airspeed	64.12 knots
I_y	12,733 slug-ft^2	R_E	78.352 ft	Rate of climb	15 fps
I_{zz}	10,800 slug-ft^2	K_c	3.46044-20.7627 (ft^2)	θ	1.39 deg
I_{xz}	1,480.4 slug-ft^2	ΔX_c	92.284 ft	ϕ	-3.5 deg
$X_{c.g.}$	141.6 in.			Density altitude	5,500 ft
$Y_{c.g.}$	0. in				
$Z_{c.g.}$	46.6 in.				

Autopilot	
Cyclic authority	10%/sec
Pedal and collective authority	10%/sec
Time to zero attitudes	0.6 sec
Time to zero rates	0.3 sec

Table 4 Comparison of vortex-induced parameter excursions

Parameter	Range of simulation results	Range of flight-test results
Station 84 flapwise bending moment	-25,000. to +33,000. in.-lb	-9,762. to 17,183. in.-lb
Station 192 chordwise bending moment	-2,000. 50 +22,000. in.-lb	-43,850. to +39,159. in.-lb
Station 192 flapwise bending moment	-1,900. to +3,200. in.-lb	-14,542. to +3,216. in.-lb
Yaw rate	7.0 left to 8.0 right deg/sec	16.1 left to 18.8 right deg/sec
Change in yaw angle	3.8 deg maximum	22.1 deg. maximum
Normal acceleration	+0.42 to +2.05 g	-0.14 to +2.0 g

V. Conclusions

Based on the flight data that were analyzed, the helicopter/vortex interaction described herein presented no safety hazards, either in vehicle response or structural loads. Specifically:

1) The maximum rotor blade strucutral loads monitored during a vortex penetration were nominal, with magnitudes less than those encountered during a 1.8 *g* turn for this test helicopter.

2) Helicopter attitude response to the vortex encounter was confined to small excursions in yaw angle.

3) Tail rotor flapping during an approach and penetration of the vortex wake was within safe operating limits, and was predominantly due to the maneuvering roll approach.

4) Separation distance between aircraft did not affect the response of the helicopter to the trailing vortex strongly.

5) Analytical simulation of this helicopter/vortex encounter can predict trends and magnitudes of the fixed-wing vortex wake effects on this helicopter's response.

References

[1]Andrews, W. H., Robinson, G. H., and Larson, R. R., "Exploratory Flight Investigation of Aircraft Response to the Wing Vortex Wake Generated by Jet Transport Aircraft," NASA TN D-6655, 1972.

[2]Dunham, R. E., Holbrook, G. T., Mantay, W. R., Campbell, R. L., and Van Gunst, R. W., "Flight Test Experience of a Helicopter Encountering an Airplane Trailing Vortex," presented to the *American Helicopter Society Forum,* Preprint 1063, May 1976.

[3]Hastings, E. C., Patterson, J. E., Jr., Shanks, R. E., Champine, R. A., Copeland, W. L., and Young, D. C., "Development and Flight Tests of Vortex-Attenuating Splines," NASA TN D-8083, 1975.

[4]Lynn, R. R., Robinson, F. D., Batra, N. N., and Duhon, J. M., "Tail Rotor Design, Part I: Aerodynamics," *Journal of the American Helicopter Society,* Vol. 15, Oct. 1970, pp. 2-15.

[5]Gessow, A. and Crim, A. D., "A Method for Studying the Transient Blade-Flapping Behavior of Lifting Rotors at Extreme Operating Conditions," NACA TN 3366, 1955.

[6]Davis, J. M. et al., "Rotorcraft Flight Simulation Program with Aeroelastic Rotor and Improved Aerodynamic Representation," U.S.A. Air Force Materials and Research Development Lab. TR 74-10A, B, C, 1974.

[7]Bennett, R. L., "Digital Computer Program DF1758, Fully-Coupled Natural Frequencies and Mode Shapes of a Helicopter Rotor Blade," NASA CR-132662, 1975.